Science and Technology Infusion Climate Bulletin
NOAA's National Weather Service
43rd NOAA Annual Climate Diagnostics and Prediction Workshop
Santa Barbara, CA, 23-25 October 2018

Understanding the Space-Varying Trends in Global Extreme Precipitation

Saman Armal and Reza Khanbilvardi
Department of Civil Engineering,
NOAA-Cooperative Center for Earth System Sciences and Remote Sensing Technologies,
Center for Water Resources and Environmental Research,
City University of New York (City College), New York, NY

1. Introduction

During the recent years, efforts have been made to investigate the time-varying trends in extreme events as one of the relevant aspects of climate change across different scales (Asadieh and Krakauer 2015; Armal *et al.* 2016; Armal *et al.* 2018a; Najafi *et al.* 2019a; Armal and Al-Suhili, 2019). Yet, there is a little understanding on space-varying trend of extreme rainfall events. For understanding the impact of anthropogenic forcing on occurrence of extremes, researchers (Sillmann *et al.* 2017; Vautard *et al.* 2016; Yiou *et al.* 2017) often separate the indirect effect on changing circulation pattern (also called dynamical process) from thermo-dynamic pathway. The dynamic process is more specific to local scale (Pfahl *et al.* 2017) and is frequently associated with regional anomalous weather pattern. However, it is fairly small compared with the uncertainty that introduced by internal climate variability (Deser *et al.* 2014). Therefore, it is more fruitful to investigate the modes of internal variability, peculiarly characterized by anomalous sea surface temperature and barometric pressure pattern especially quasi-periodically oscillations indices *e.g.* El Niño/Southern Oscillation (ENSO), the Pacific Decadal Oscillation (PDO), the North Atlantic Oscillation (NAO) and other so-called modes of variability (Hartmann *et al.* 2013; Trenberth *et al.* 2015; Najafi *et al.* 2018a; Najafi *et al.* 2018b; Najafi *et al.* 2018c; Armal *et al.* 2018b; Najafi *et al.* 2019b). This study extracts and validates an index to study the space-varying trends in simultaneous extreme precipitation events. It correlates the frequency of simultaneous extremes with Global Surface Anomaly Temperature (GST) as a proxy of thermodynamic pathway, and a number of climate variability modes (ENSO, NAO, PDO and AMO), as a proxy of internal climate variability.

2. Methodology

In a few examples of applying spatial indices, researchers either look at the grids with highest and lowest 30% of the values, associated with the number of wet and dry grids, in each year of global data (Donat *et al.* 2016) or rely on the high percentile index of daily data over limited spatial extent (Fischer and Knutti 2015). The global ratio of daily extremes (GRDE) is designed to aggregate in-situ extremes over space. For each day of data, we consider the total number of stations with rainfall events exceeding a threshold of 99% of the full period. The product data is a time-series of daily total number of stations which are showing a value above 99% threshold. To minimize the effect of data scarcity in our analysis, the number of stations with extreme events is divided by the number of stations with available data:

$$GRDE_d = \frac{\sum_{i=1}^{NS} \delta_{id}}{NS} \quad , \quad \delta_{id}^{j} = \begin{cases} 1 & if \quad P_{id}^{j} \geq P_i^* \\ 0 & if \quad P_{id}^{j} < P_i^* \end{cases}$$

where *d* is the day index, *i* is the numerator index for stations with available data, P_{id}^{j} is the j^{th} daily rainfall of station *i* in a year, and P_i^* is the rainfall exceeding threshold for that station. *NS* is the total number of stations with available data in the day *d*. δ is the binary indicator function.

At first, we implement GRDE aggregation over different continents to extract the top 20 days with higher values. These dates are applied to daily composites of perceptible water content (PWC) anomalies (mean - total

Correspondence to: Saman Armal, Department of Civil Engineering, NOAA-Cooperative Center for Earth System Sciences and Remote Sensing Technologies, Center for Water Resources and Environmental Research, City University of New York (City College), New York, NY 10031; E-mail: sarmal000@citymail.cuny.edu

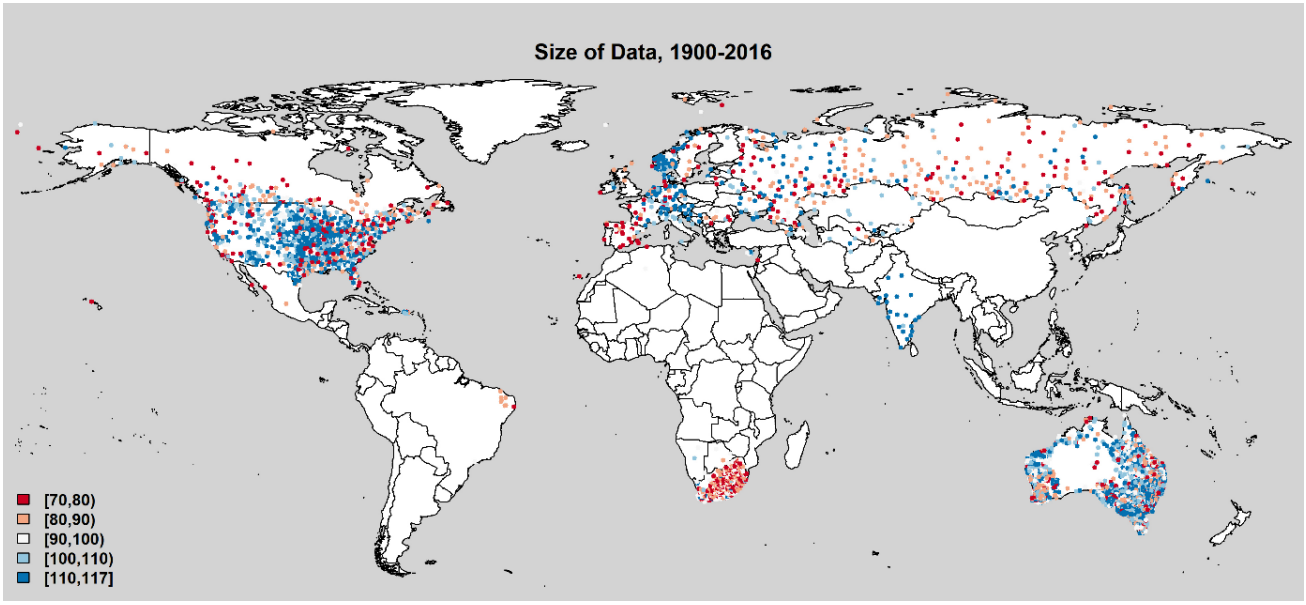

Fig. 1 We looked at more than 100,000 GHCN (Global Historical Climatology Network - daily database https://www.ncdc.noaa.gov/oa/climate/ghcn-daily/) stations across the globe and extracted the total daily precipitation from those that have data from 1900 - 2016 (117 years). From this data, we selected high-quality stations using the following procedure. First, for each year, if more than 40% of days is missing data, we flag this as a missing year. Next, only stations that have at least 70 years of complete data are selected. This process yielded 6185 stations across the globe.

mean) to perceive whether there is any distinctive circulation pattern over the region (note that the historical climate data starts from 1948, hence the selected dates for composite maps are limited to this period). Moreover, these patterns are compared to the global spatial distribution of stations that experience at least one extreme in the top 20 dates. The extent of anomalous PWC yields information about the occurrence of extremes in rest of the world.

Also, we apply Generalized Extreme Value (GEV) fit distribution on yearly maximum GRDE and inform the location parameters with GST as an indicator for thermodynamic pathway and ENSO, NAO, PDO and AMO as an indicator for dynamical process.

$$GRDE_{y,max} \sim GEV\left(\mu_y \mid GST + ENSO + NAO + PDO + AMO, \sigma, \varepsilon\right)$$

Here μ_y is the location parameter, σ is the scale parameter and ε is the shape parameter. For every continent as well as Northern/Southern hemisphere, we randomly chose 100 blocks with 60-yr size of data, and performed the GEV fit distribution. Furthermore, we exclude the all the estimations which are outside the 95 confidence interval.

3. Results

We present the results of our analysis for three continents: North America, Europe and Australia. Figure 2 indicates the location of global stations that shows at least one day of extreme precipitation in the top 20 GRDE. Fig. 2-a is based on the top 20 days with highest percentage of simultaneous extreme events in North America, Fig. 2-b is based on Europe and Fig. 3-c is based on Australia.

The PWC composite maps identify the anomaly of total water content in the selected days. Unlike Europe, both North America and Australia confirm the occurrence of wide spread extreme rainfall with positive anomaly values of PWC. Notably, in the top 20 GRDE of North America many stations flags with extreme rainfall in Australia. Reciprocally, the same feature is observed in North-west America, in the top 20 GRDE days of Australia. Another possible linkage is evident in the top 20 GRDE of Europe, when many stations in North America are identified with an extreme rainfall. The PWC maps suggest spread of spatial anomalous field across

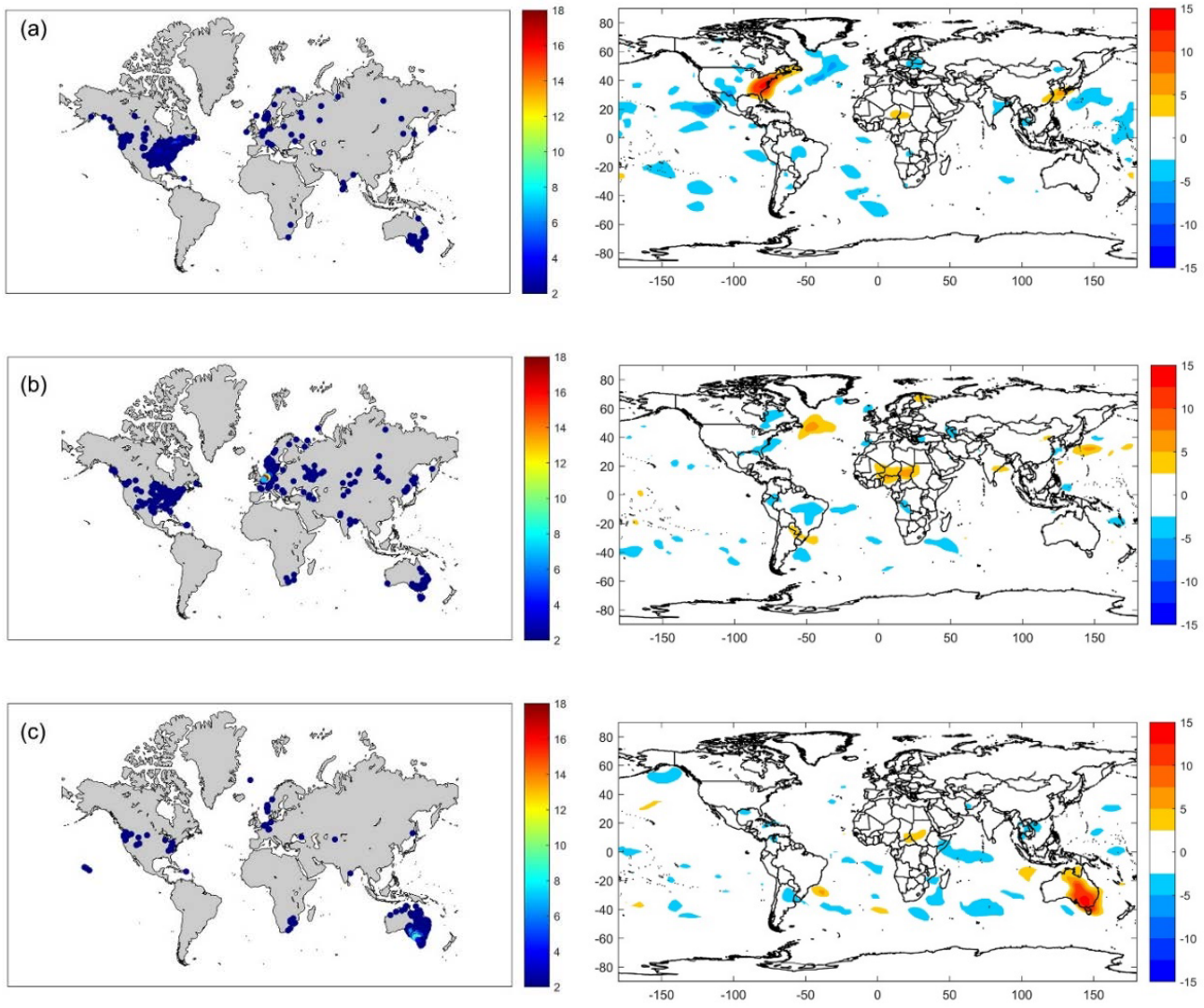

Fig. 2 Continent-based maps of stations with at least one event in the first 20 days of with highest GRDE for (a) North America, (b) Europe and (c) Australia. The corresponding anomaly maps on the right indicate the anomaly of perceptible water content (kg/m^2) in the respective days.

the globe, with no significant impact over Europe. The number of extremes is concentrated over relatively small area and induced by few number of stations.

Figure 3 shows the values obtained for location parameters for different continents. This values are obtained from 100 bootstrapping block over GEV analysis. None of the results suggest the impact of high to medium frequency modes of climate variability on the occurrence of simultaneous extreme rainfall. In Europe/Australia, there is a strong positive/negative correlation between trend in GRDE and global surface temperature anomaly. The response of North America to GST highly varies but the median is close to zero. Moreover, in North America/Australia, positive/negative AMO links to frequency of the simultaneous extreme events. The linkage of AMO variation with strength of Thermohaline Circulation (THM) (García‐García and Ummenhofer 2015) can regulate the climate across the globe and impact the occurrence of global extremes.

References

Armal, S., N. Devineni, and R. Khanbilvardi, 2016: multilevel Poisson regression model to detect trends in frequency of extreme rainfall events. *American Geophysical Union Fall Meeting 2016*, San Francisco, CA, USA, 12–16 December 2016, AGU, Abstract #NH51B-1957.

—, —, and —, 2018a: Trends in extreme rainfall frequency in the contiguous United States: Attribution to climate change and climate variability modes. *J. Climate*, **31**, 369–385, doi:10.1175/JCLI-D-17-0106.1.

—, —, and —, 2018b: New York city's water system performance analysis based on current and projected demands. *American Geophysical Union Fall Meeting 2018*, Washington, DC, USA, 10–14 December 2018, AGU, Abstract #H41I-2167.

— and R. Al-Suhili, 2019: An urban flood inundation model based on cellular automata. *International Journal of Water, in press.*

Asadieh, B., and N. Y. Krakauer, 2015: Global trends in extreme precipitation: Climate models versus observations, *Hydrol. Earth Syst. Sci.*, **19**, 877–891, doi:10.5194/hess-19-877-2015.

Deser, C., and Coauthors, 2014: Projecting North American climate over the next 50 years: Uncertainty due to internal variability, *J. Climate*, **27**, 2271–2296, doi:10.1175/JCLI-D-13-00451.1.

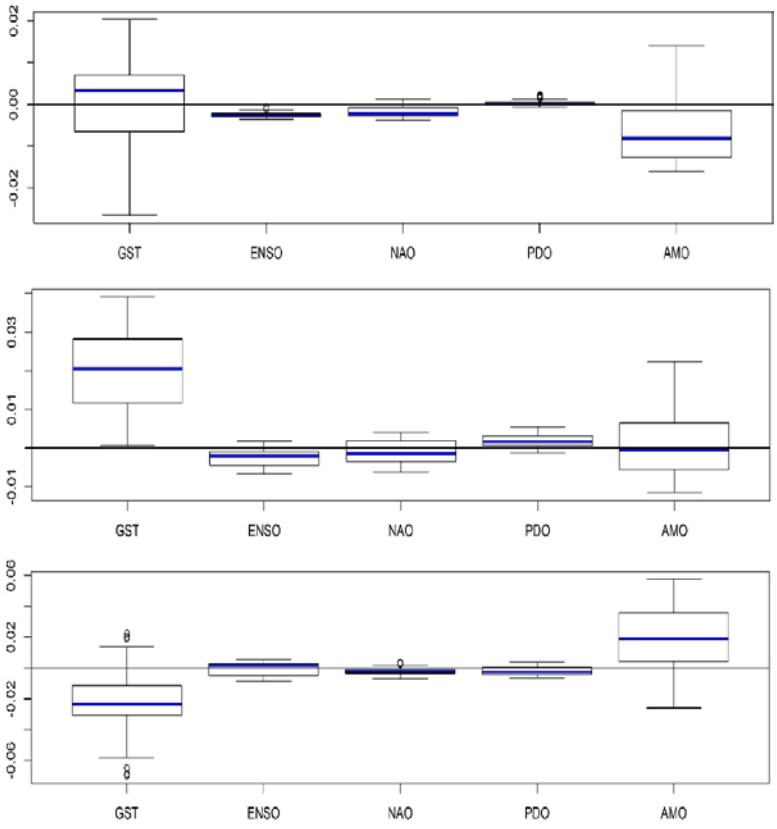

Fig. 3 The values of GEV location parameters for North America (top), Europe (middle), and Australia (bottom).

Donat, M. G., and Coauthors, 2016: More extreme precipitation in the world's dry and wet regions, *Nature Climate Change*, **6**, 508–513, doi:10.1038/nclimate2941.

Fischer, E. M., and R. Knutti, 2015: Anthropogenic contribution to global occurrence of heavy-precipitation and high-temperature extremes, *Nature Climate Change*, **5**, 560–564, doi:10.1038/nclimate2617.

García-García, D. and C. C. Ummenhofer, 2015: Multidecadal variability of the continental precipitation annual amplitude driven by AMO and ENSO, *Geophys. Res. Lett.*, **42**, 526–535, doi:10.1002/2014GL062451

Hartmann, D. L., and Coauthors, 2013: Observations: Atmosphere and surface. *Climate Change 2013: The Physical Science Basis. Contribution of Working Group I to the Fifth Assessment Report of the Intergovernmental Panel on Climate Change*, T. F. Stocker, D. Qin, G.-K. Plattner, M. Tignor, S. K. Allen, J. Boschung, A. Nauels, Y. Xia, V. Bex and P. M. Midgley, Eds., Cambridge University Press, 159–254, doi:10.1017/CBO9781107415324.008.

Najafi, E and R. Khanbilvardi, 2018a: Clustering and trend analysis of global extreme droughts from 1900 to 2014, https://arxiv.org/pdf/1901.00052v2

—, I. Pal, and R. Khanbilvardi, 2018b: Diagnosing extreme drought characteristics across the globe. *NWS Sci. Technol. Infusion Clim. Bull., 42nd NOAA Annu. Clim. Diagn. Predict. Workshop*, 121-125, doi:10.7289/V5/CDPW-NWS-42nd-2018.

—, N. Devineni, R. M. Khanbilvardi, and F. Kogan, 2018c: Understanding the changes in global crop yields through changes in climate and technology. *Earth's Future*, **6**, 410-427, doi:10.1002/2017EF000690

—, I. Pal, and R. Khanbilvardi, 2019a: Climate drives variability and joint variability of global crop yields. *Sci. Total Environ*, **662**, 361–372.

—, —, and —, 2019b: Data of variability and joint variability of global crop yields and their association with climate. *Data in Brief*, **23**, 103,745, doi: https://doi.org/10.1016/j.dib.2019.103745.

Pfahl, S., P. A. O'Gorman, and E. M. Fischer, 2017: Understanding the regional pattern of projected future changes in extreme precipitation, *Nature Climate Change*, **7**, 423–427, doi:10.1038/nclimate3287.

Sillmann, J., and Coauthors, 2017: Understanding, modeling and predicting weather and climate extremes: Challenges and opportunities, *Weather and Climate Extremes*. 18, 65-74, doi:10.1016/j.wace.2017.10.003.

Trenberth, K. E., J. T. Fasullo, and T. G. Shepherd, 2015: Attribution of climate extreme events, *Nature Climate Change*, **5**, 725–730, doi: 10.1038/nclimate2657.

Vautard, R., and Coauthors, 2016: Attribution of human-induced dynamical and thermodynamical contributions in extreme weather events, *Environ. Res. Lett.*, **11**. 1-9, doi:10.1088/1748-9326/11/11/114009.

Yiou, P., and Coauthors, 2017: A statistical framework for conditional extreme event attribution, *Adv. Stat. Clim., Meteorol. Oceanogr.*, **3**, 17–31. doi:10.5194/ascmo-3-17-2017.